

Conf-941142--34

PNL-SA-24240

TURBULENCE PRODUCTION IN FLOW NEAR A WAVY WALL

J. D. Hudson
L. Dykhno^(a)
T. J. Hanratty^(a)

November 1994

Presented at the
International Mechanical Engineering Congress and Exposition:
Turbulence in Complex Flow
November 7, 1994
Chicago, Illinois

Prepared for:
the U.S. Department of Energy
under Contract DE-AC06-76RLO 1830

Pacific Northwest Laboratory
Richland, Washington 99352

(a) University of Illinois, Urbana, Illinois

DISCLAIMER

This report was prepared as an account of work sponsored by an agency of the United States Government. Neither the United States Government nor any agency thereof, nor any of their employees, makes any warranty, express or implied, or assumes any legal liability or responsibility for the accuracy, completeness, or usefulness of any information, apparatus, product, or process disclosed, or represents that its use would not infringe privately owned rights. Reference herein to any specific commercial product, process, or service by trade name, trademark, manufacturer, or otherwise does not necessarily constitute or imply its endorsement, recommendation, or favoring by the United States Government or any agency thereof. The views and opinions of authors expressed herein do not necessarily state or reflect those of the United States Government or any agency thereof.

MASTER

DISTRIBUTION OF THIS DOCUMENT IS UNLIMITED

DISCLAIMER

**Portions of this document may be illegible
in electronic image products. Images are
produced from the best available original
document.**

TURBULENCE PRODUCTION IN FLOW NEAR A WAVY WALL

John D. Hudson
Fluid Dynamics Laboratory
Pacific Northwest Laboratory*
Richland, Washington 99352

Leonid Dykhn and Thomas J. Hanratty
Department of Chemical Engineering, University of Illinois
Urbana, IL 61801

ABSTRACT

Measurements of the spatial and time variation of two components of the velocity have been made over a sinusoidal solid wavy boundary with a height to length ratio of $2a/\lambda = 0.10$ and with a dimensionless wave number of $\alpha^+ = 0.02$. For these conditions, both intermittent and time-mean flow reversals are observed near the troughs of the waves. Statistical quantities that are determined are the mean streamwise and normal velocities, the root-mean-square of the fluctuations of the streamwise and normal velocities, and the Reynolds shear stresses. Turbulence production is calculated from these measurements.

The flow is characterized by an outer flow and by an inner flow extending to distance of about α^{-1} from the mean level of the surface. Turbulence production in the inner region is fundamentally different from flow over a flat surface in that it is mainly associated with a shear layer that separates from the back of the wave. Flow close to the surface is best described as an interaction between the shear layer and the wall, which produces a retarded zone and a boundary-layer with large wall shear stresses.

Measurements of the outer flow compares favorably with measurements of over a flat wall if velocities are made dimensionless by a friction velocity defined with a shear stress obtained by extrapolating measurements of the Reynolds stress to the mean levels of the surface (rather than from the drag on the wall).

I. INTRODUCTION

If a turbulent fluid passes over a periodic train of solid waves with large enough steepnesses (wave height to length ratio), separated regions with a time-mean reversed flow can exist in the troughs. An understanding of this flow has been a continuing interest of this laboratory.

Zilker & Hanratty (1979) measured the variation of the surface stress along a solid wavy boundary with

electrochemical probes. Buckles et al (1994) used a single-component laser-Doppler system to measure the time mean velocity, \bar{U} , and the root-mean-square of the velocity fluctuations, $\overline{u^2}$, in the streamwise direction. They found a layering of the maxima in $\overline{u^2}$ associated with the formation of shear layers behind the crests of the waves. The flow over each wave was described as consisting of four zones: an outer flow, a shear layer, a separated region and a thin boundary-layer which is initiated close to the point where the separated flow reattaches to the surface. Kuzan et al (1989) used the LDV developed by Buckles to investigate the transition from a turbulent separated flow to a turbulent non-separated flow with increasing Reynolds number.

McLean (1983) developed a computational method to calculate the behavior of a turbulent boundary-layer in the presence of a train of solid waves. Kuzan et al (1989) and Frederick & Hanratty (1988) modified the code for flow in an enclosed channel. Both computations employed models for the Reynolds shear stress based on studies of turbulent flow over a flat plate. The agreement between the calculations and measurements appear to be reasonable. However, a closer examination by Kuzan et al (1989) and by Frederick & Hanratty (1988) reveals serious shortcomings.

The present study is an extension of the work by Buckles and by Kuzan in that two components of the velocity field are measured. The principal motivation for the study is the need to test models for Reynolds stress directly rather than, indirectly, through measurements of the mean flow field. The focus of the present paper is to provide a phenomenological understanding of the flow which could be a basis for analysis.

A principal finding is that turbulence production near the boundary is fundamentally different from flow over a flat wall in that it is associated with a separating shear layer. Production by flow oriented vortices such as found for flat walls (Brooke & Hanratty [1993], Kline & Robinson [1989]) appears to be unimportant. However, turbulence quantities in

the outer flow are the same, if scaled with an appropriate friction velocity. This suggests that the outer flow could have a universal character, independent of how it is produced at the wall.

II. EXPERIMENTAL

The measurements were made in a rectangular water channel with a cross section of 5.08×61 cm. The test section was preceded by approximately 100 channel heights to insure a fully developed flow. The lower wall was constructed with removable Plexiglas plates on which were milled sinusoidal waves of length 5.08 cm and amplitude 0.254 cm. The measurements were made above the 31st of 36 waves to insure a fully periodic flow field. Details on the channel construction are given by Niederschulte (1988).

The LDV system used in the experiments is described by Niederschulte et al. It consisted of a 35 mW Spectra Physics He-Ne laser and TSI optics which used polarization rotation to achieve channel separation. The three beam, two component system was operated in the forward scatter mode. Flow reversals were detected by the use of a Bragg (acousto-optic) cell with electronic downmixing.

Two TSI IFA 550 signal processor performed the signal validation and recording. A dedicated IBM PC/AT controlled the processing, acquisition and intermediate data storage. These data were later transfer to a Digital DecStation 5000/200 for statistical analysis. Sets of 30,000 instantaneous pointwise measurements of two components of the fluid velocity were obtained at 50 locations normal to the wave surface (from near the wave surface to the channel center) and at 10 streamwise locations.

The time between measurements (2 ms) was short compared with the characteristic period of turbulence; the period over which the measurements were taken (60 s) was longer than the characteristic period of turbulence. Statistical quantities that were calculated include the mean streamwise, \bar{U} , and normal, \bar{V} , velocities, the root-mean-square (rms) values of the streamwise, $(\bar{u}^2)^{1/2}$, and normal, $(\bar{v}^2)^{1/2}$, turbulent velocity fluctuations and the mean Reynolds shear stress \bar{uv} . Other properties of interest are calculated from these mean values and their derivatives.

The wave steepness was $2a/\lambda = 0.1$. The Reynolds number $Re_h = \langle U_b \rangle h / v$, with $\langle U_b \rangle$ being a wave-averaged bulk velocity, was set at 3340 so as to be in a region where separation occurs, according to the map of Zilker (1979). All the measurements of \bar{U} , \bar{V} , $(\bar{u}^2)^{1/2}$, $(\bar{v}^2)^{1/2}$ and \bar{uv} are tabulated in the thesis by Hudson (1993).

III. RESULTS FOR THE OUTER FLOW

Figure 1 presents distributions of the streamwise and normal mean velocities at 10 locations along the wave. These velocities are normalized by a friction velocity (u_w^*) which is defined from the Reynolds stress measurements (Eqn. 4). The abscissa gives the distance from reference height y_0 , made dimensionless with the channel half-height. This reference is chosen as the mean location of the wavy surface so that the measurements of τ_t extrapolate to the wall drag at $y-y_0=0$ (Hudson¹⁰). The variation of these velocities about the wave-

averaged mean is small for $(y-y_0)/h > 0.3$, which is described as the inner region.

Inner and outer regions can also be recognized from profiles of the turbulent velocity fluctuations and the Reynolds stress, which are presented in Figure 2. As with the mean streamwise velocities, the boundary between an inner and an outer region is near $(y-y_0)/h \approx 0.3$. The inner is characterized by large spatial variations of the turbulence and distinct maxima. There are small wave-induced variations in \bar{u}^2 and \bar{v}^2 in the outer region; these quantities are affected only indirectly (through the value of u_w^*) by the presence of the wavy surface. The magnitudes of the turbulence quantities slowly decrease with distance from the wave to the values at the channel center. The maximum values of the dimensionless streamwise (2.5) and normal (1.25) turbulent velocity fluctuations and the Reynolds shear (1.6) stress occur near $(y-y_0)/h=0.1$.

A description of the outer flow requires an appropriate velocity scale analogous to the friction velocity defined for flow over a flat plate or over a small amplitude wave,

$$\frac{u_{fl}^*}{\langle U_B \rangle} = \sqrt{\frac{0.0612 Re_h^{-0.25}}{2}}, \quad (1)$$

where $\langle U_B \rangle$ is the bulk velocity given by

$$\langle U_B \rangle = \frac{\frac{\lambda h}{\lambda h} \iint \bar{U} dy dx}{\frac{00}{00} \iint dy dx}. \quad (2)$$

For the flow over a large amplitude wave this relation gives a velocity scale which is too small.

The measurement of Reynolds shear stresses allows direct calculation of a more appropriate friction velocity, u_w^* . A shear stress τ which includes both the Reynolds shear stress and the viscous shear stress is defined by

$$\tau^+ = \frac{v}{u_{fl}^{*2}} \frac{d\bar{U}}{dy} - \frac{\bar{uv}}{u_{fl}^{*2}}, \quad (3)$$

where τ^+ is made dimensionless with ρu_{fl}^{*2} . The averages of τ^+ over a wavelength, $\langle \tau^+ \rangle$, are presented as the open symbols in Figures 3. The approximately linear variation in the outer region indicates these data can be used to define

$$u_w^* = \frac{y-y_0}{\rho}, \quad (4)$$

extrapolating to $y=y_0$. A value of $u_w^{*2} = 2.91 u_{fl}^{*2}$ is obtained in this way. From an extrapolation toward the channel center, the zero value of τ is located near $y-y_0/h=1.3$. Since $u_{fl}^* = 0.76$ cm/s, a value of $u_w^* = 1.30$ cm/s is obtained. This is approximately 60% higher than the friction velocity

for a flow over a flat plate at the same Re_h .

Another possible choice of the velocity scale may be defined from the wave-averaged total drag. Mean velocities \bar{U} and \bar{V} , although small, make significant contributions to momentum transport. The phase relation of the two quantities is such that the wavelength average of $-\rho \langle \bar{U} \bar{V} \rangle$ is not zero. Consequently,

$$\langle \bar{U} \bar{V} \rangle = \frac{1}{\lambda} \int_0^\lambda (\bar{U} \bar{V}) dx, \quad (5)$$

is not zero. This contributes to a net momentum flow in the y -direction or an effective stress equal to $-\rho \langle \bar{U} \bar{V} \rangle$. A total shearing stress τ_t may be defined by

$$\tau_t^+ = \frac{v}{u_{fl}^{*2}} \frac{d\bar{U}}{dy} - \frac{\bar{u}\bar{v}}{u_{fl}^{*2}} - \frac{\bar{U}\bar{V}}{u_{fl}^{*2}}. \quad (6)$$

The wave-averaged mean total effective stresses $\langle \tau_t^+ \rangle$ are presented as the closed symbols in Figure 3. A straight line fit of these data extrapolates to a value of $4.3 \pm 0.5 u_{fl}^{*2}$ at $y=y_0$ and to zero near $(y-y_0)/h=1.3$. The square-root of the value at $y=y_0$ gives $u_t^* = 1.58$ cm/s, which is twice the flat channel friction velocity u_{fl}^* . This intercept is the dimensionless drag of the wall given by $(D/\lambda W)(1/u_{fl}^{*2})$, where D is the drag force.

The turbulent velocity fluctuations and the Reynolds shear stresses normalized by the friction velocity u_w^* are compared to the data obtained with a flat channel by Niederschulte et al. at a similar Reynolds number ($Re_h=2470$) in Figure 2 (the solid curves). The dimensionless streamwise turbulent velocity fluctuations for the wavy surface are close to the values for a flat wall; the normal fluctuations and Reynolds shear stresses are slightly higher. Somewhat better agreement could be obtained by offsetting the flat channel data slightly from the wavy surface (approximately $\Delta y/h=0.2$) so that the zero-stress location for the flat plate (the channel center, or $y-y_0/h=1.0$) and the zero-stress location for the wavy surface (approximately $y-y_0/h=1.2$ as defined by Figure 3) coincide. The good agreement between the data for the flat and wavy walls in Figure 2 indicates that u_w^* is an approximate scaling for these quantities.

The effects of the wavy surface on the wave-averaged velocities are felt in the log-law region through the change in the friction velocity u_w^* . The wave-averaged mean streamwise velocities in the outer flow region are presented in Figure 4. These velocities agree well with the equation

$$\frac{\bar{U}}{u_w^*} = \frac{e}{\kappa} \log \frac{(y-y_0)u_w^*}{v} - 2.94 \quad (7)$$

(shown as a solid line) with the region $50 < (y-y_0)u_w^*/v < 150$. The coefficient which describes these data is the same used for a flat channel; $e/\kappa=5.75$, where e is the natural logarithm constant and κ is von Karman's constant.

These data also agree well with an equation of the form

$$\frac{\bar{U}}{u_w^*} = \frac{e}{\kappa} \log \frac{y-y_0}{k_s} + B, \quad (8)$$

suggested by Schlichting (1979) to describe the outer flow region above a roughened surface. An equivalent sand roughness for the wavy surface of 0.5 cm is calculated from Eqn. 8 by using $(e/\kappa)=5.75$ and $B=8.6$. This roughness is approximately the total wave height $2a=0.51$ cm. The dimensionless equivalent sand roughness, $k_s^+ = k_s u_w^*/v$, therefore, is on the order of 70. This is near the value for a completely rough surface as defined by Nikuradse, justifying the use of $B=8.6$.

The slope of the streamwise log-layer data normalized by the friction velocity u_w^* is consistent with the e/κ slope obtained for a variety of wall bounded flows. For an alternate choice of the friction velocity, such as u_t^* , the value of the

von Karman constant κ would be defined as $\kappa \left(\frac{u_t^*}{u_w^*} \right)$ for a good fit of the data. That is, it would require a 20% increase in the accepted value of κ if $u_t^*=1.58$ cm/s is used instead of u_w^* . This observation, along with the good agreement of the measurements of the turbulence quantities in Figure 2 with the results of Niederschulte, is used as a justification for the choice of u_w^* as the velocity scale.

IV. INNER REGION

A. Features of the inner region

The main focus of this paper is the inner region where the effects of the wavy wall are the most evident. Following the discussion of Buckles, et al², the flow features are described by considering it to consist of a separated region, a boundary layer and a shear layer.

The mean velocity field in the inner region is presented in Figure 5 in vector form and as streamlines, obtained by integration of the mean streamwise velocities

$$\psi(x, y') = \int_0^y \bar{U}(x, y') dy' \quad (9)$$

where y' is the distance above the wave surface at a given x . Contours of the mean Reynolds shear stress are presented in Figure 6.

The separated region is bounded by the $\psi=0$ streamline and the wavy boundary between $x/\lambda=0.3$ and $x/\lambda=0.5$. A region of large velocity gradients close to the wall, called a boundary layer, forms immediately downstream of the separation region

(near $x/\lambda = 0.6$) and extends almost to the next wave crest. The boundary upstream of the crest is influenced by the accelerating outer flow, that is, a favorable gradient of $(p + \overline{u^2})$. It has a thickness of the order of 1 mm. As the boundary layer thickens, instabilities occur when the fluid near the wall begins to decelerate. These instabilities grow in the presence of the adverse gradient of $(p + \overline{u^2})$ which occurs beyond $x/\lambda = 0.9$. Downstream of the crest, the flow at the wall separates. As seen in Figure 5, an inflection point with a large velocity gradient develops away from the wall. The region surrounding this inflectional point is called a "shear layer"; it resembles a classical free shear layer or mixing layer. This layer begins close to the wavy surface near $x/\lambda = 0.1$ and develops downstream so that its effects are experienced for several wavelengths. Its outer extent can be defined by an outer inflectional point in the mean velocity profiles. The center of the shear layer is defined by the loci of maxima in the Reynolds shear stress, shown as a dashed line in Figure 6. The lower part of the shear layer differs considerably from the upper part because of the interaction with wall. The definition of this interaction emerges as a critical theoretical problem. In fact, the separated region and the boundary layer may be considered as manifestations of this interaction.

B. The Reynolds shear stress

The time-averaged Reynolds shear stresses are presented as contours in Figure 6. The abscissa is the distance from the crest in the streamwise direction normalized by the wavelength λ . The contour values are made dimensionless with the friction velocity u_w^* .

As Figure 6 indicates, the values of the time-averaged Reynolds shear stress vary from a maximum just above 1.6 to small negative values. The areas of negative stresses which occur on the upstream and downstream sides of the wave are artifacts of calculating the Reynolds shear stress in a Cartesian coordinate system. As is shown in the thesis of Hudson (1993), Reynolds shear stresses assume positive values in these regions if they are calculated in a boundary-layer coordinate system.

A region of maximum values of the time-average Reynolds shear stress begins to develop near $x/\lambda = 0.1$, $(y-y_0)/h = 0.1$ with a value of approximately 0.5. Downstream it rapidly increases in extent until it reaches a global maximum (1.66) at $x/\lambda = 0.5$. The region may be traced far downstream well beyond the next crest.

The loci of Reynolds shear stress maxima (shown as the dashed line of Figure 6) coincides approximately with a characteristic inflection in the velocity profile at the center of the shear layer. Because this inflection is, in some places, broad and because the velocity profile is not symmetric about the shear layer center for every streamwise location, the loci of shear stress maxima provide more convenient markers of the location of the shear layer.

The overall variation of the Reynolds shear stress is large. This may be seen in the streamwise direction along a line near $(y-y_0)/h = 0.1$, where the minimum value is approximately 0.3 at $x/\lambda = 0.0$ and the maximum value is larger than 1.6 (at $x/\lambda = 0.5$). In the normal direction the variation is also large.

This is particularly evident $x/\lambda = 0.4$ and $x/\lambda = 0.6$ where the values decrease monotonically from the maximum value of 1.2-1.4 (near $(y-y_0)/h = 0.1$) to near zero close to the wavy surface.

Near the wavy surface the Reynolds stress varies roughly with the distance from the surface. Consequently the contours of constant stress are roughly parallel to the boundary. Near the center of the shear layer the Reynolds stresses at different locations along the shear layer vary roughly with distance from the center normalized by a length describing the shear layer extent. In the outer region the Reynolds shear stress is approximately a constant at a constant $(y-y_0)$. (See also the bottom of Figure 2.)

C. Turbulent energy production

The time-averaged mean rate of turbulent kinetic energy production, \dot{E}_{tk} , is given by the following equation if the mean flow and the turbulence do not vary in the x_2 -direction:

$$\dot{E}_{tk} = -\overline{uv}\frac{\partial \bar{U}}{\partial y} - \overline{u^2}\frac{\partial \bar{U}}{\partial x} - \overline{vu}\frac{\partial \bar{V}}{\partial x} - \overline{v^2}\frac{\partial \bar{V}}{\partial y} \quad (10)$$

Here the turbulent kinetic energy per unit mass is defined as $(\overline{u^2} + \overline{v^2})/2$. The first two terms represent a direct transfer of energy from the mean flow to the streamwise component of the turbulent kinetic energy $(\overline{u^2}/2)$. The third and fourth represent a direct transfer to $(\overline{v^2}/2)$. For flow above a flat plate the last three terms in Eqn. 10 are zero as the gradients in the time-averaged mean velocity are zero. However, these terms may be important near a wavy surface where the wave-induced flows are associated with large gradients of u and v in both the x - and y -directions.

The turbulent kinetic energy production, defined by Eqn. 10, was made dimensionless with u_w^{*4}/v and is presented for the flow at $Re_h = 3380$ as the contours of Figure 7. The contributions of the four terms in Eqn. 10 are presented in Figure 8, where the dashed contours indicate negative values of the contribution. While the first term $(-\overline{uv}\partial \bar{U}/\partial y)$ is still dominant throughout most of the two-dimensional field, the second term $(-\overline{u^2}\partial \bar{U}/\partial x)$ in some places, is the same order as the first. This is particularly evident in the downstream region of the wave where the relatively large negative values of the second term tend to balance the positive values of the first term. The maximum positive value (0.15) of the second term occurs just above the crest in the same area as the maximum values of the first term (0.30). Thus, the second term contributes approximately 35% of the total production in the area near the locus of maximum total production. A large region of negative contribution of the second term occurs in the downstream half of the wave near $x/\lambda = 0.6$, $(y-y_0)/h = 0.75$. These negative values tend to offset the positive values of the first and fourth term so that the total production in the region is near zero. The fourth term $(\overline{v^2}\partial \bar{V}/\partial y)$ has significant magnitudes only in the downstream region, near the wavy

surface. The positive values of the fourth term balance the slightly negative values of the first term very close to the wavy surface, downstream of the reattachment point and balance, to some extent, the negative values of the second term. The third term production $(-\bar{v}u \frac{\partial \bar{V}}{\partial x})$ contributes a significant part of the total production only in a very small area near its maximum (0.013), which is near $x/\lambda=0.65$ ($y-y_0)/h=0.10$), where the other three terms are small.

While the first production term may be considered a rough estimate of the total turbulent kinetic energy production, the consideration of the second and four term are required for an accurate representation of the magnitudes and locations of maxima and minima. This is particularly true very near the wall (from $x/\lambda \approx 0.5$ to $x \approx 0.8$) where the first term gives negative values and in the downstream regions where the first, second and fourth terms are of the same order.

As shown in Figure 7, large values of the production are associated with the downstream part of the boundary layer and with the development of the shear layer, particularly in the area of its initiation. These large values precede the crest (near the surface at $x/\lambda=0.9$) and continue downstream roughly following the developing shear layer. Past reattachment the production associated with the shear layer has values less than 0.05.

A large area of near zero production occurs near the surface. This area begins near the formation of the separated region (at $x/\lambda=0.2$) and continues downstream through most of the boundary layer development past ($x/\lambda=0.8$).

D. The mean turbulent velocity fluctuations

The root-mean-square of the streamwise and normal turbulent velocity fluctuations, made dimensionless with u_w^* , are presented as contours in Figure 9. The mean streamwise fluctuations are characterized by large magnitudes throughout the inner region, except very close to wall where the values decrease to zero. The most prominent feature of this field is the large region encompassing the maximum values. This region begins near the wall at approximately $x/\lambda=0.8$. (See the contour with a value of 1.8, Figure 9, top), continues over the crest, and broadens, attaining a maximum value of 2.5 at $x/\lambda=0.5$, ($y-y_0)/h=0.1$. The band continues downstream narrowing as it approaches the next crest, where two maxima are shown (1.8 at $y-y_0/h=0.12$ and 1.8 at $y-y_0/h=0.23$). This region may be followed past the crest where its value decreases. Eventually the band cannot be differentiated from the outer flow values (1.2-1.4).

As pointed out by Buckles (1984), the loci of maxima in this region correspond roughly to inflections in the mean velocity profile and, therefore, to the center of the shear layer from approximately $x/\lambda=0.2$ downstream. However, the region of maxima in u_{rms} starts close to the wall near $x/\lambda=0.8$. This location corresponds to the maxima in turbulent kinetic energy production shown in Figure 7. This behavior may be associated with the shear layer interacting with the rising surface contour.

The variation in the values of the streamwise root-mean-square

(rms) fluctuations in the separated region is different from what is observed for the kinetic energy production. The values decrease monotonically from those found in the shear layer (≥ 1.5) to near zero close to the wavy surface. However, u_{rms} has finite values in the separated region, even though the turbulent energy production is zero. A similar behavior is observed near the wall from $x/\lambda=0.5$ to $x/\lambda=0.8$. This indicates that the energy is convected or diffused from above rather than produced locally. The overall variation of the streamwise fluctuations is relatively small throughout the entire inner region. In the streamwise direction the maximum variation is approximately 25% of the maximum, from 1.8 to 2.4 at ($y-y_0)=0.1$.

The variation in the normal fluctuations is similar to that of the streamwise fluctuations. The overall variation is small, particularly in the streamwise direction where the maximum variation of 0.4 to 1.2 occurs along ($y-y_0)=0.1$. However, there are some differences.

The region of maxima in the normal fluctuations lags that of the streamwise fluctuations. In the area where the streamwise fluctuations are initiated and the turbulent kinetic energy production is a maximum (near $x/\lambda=0$), ($y-y_0)/h=0.02$, Figure 7), the normal rms values are low. Furthermore, only a single maximum is shown at $x/\lambda=1.0$; this maximum corresponds roughly to the center of the shear layer. The initiation of the region of maxima normal rms, values occurs near $x/\lambda=0.3$, ($y-y_0)/h=0.07$ where the value is approximately 0.8. The normal fluctuations increase in magnitude to a maximum which occurs at $x/\lambda=0.6$, where its value is 1.25. Like the streamwise fluctuations, the region of maxima of normal rms values can be traced some distance downstream, extending beyond the next crest. The values downstream decrease to values close to that in the outer flow, 0.6-0.7. However, it is noted that the loci of maxima in v_{rms} occurs below the loci of maxima in u_{rms} . This could be associated with the energy production results shown in Figure 8, as the maximum direct production of $(\bar{v}^2/2)$, by terms three and four, occurs in the region where v_{rms} is the largest. But, since these production terms are quite small, this suggestion must be regarded as speculative.

The lag that is observed in the maxima of normal rms values with respect to the streamwise rms values is another indication that the turbulence production process is initially characterized by large fluctuations in the streamwise direction. Significant fluctuations in the normal direction occur downstream; these result from flow structures spawned by the large streamwise fluctuations. These results are also consistent with the equations which describe the balance of turbulent kinetic

energy. These show that $\bar{u}v \frac{\partial \bar{U}}{\partial y}$ and $\bar{u}^2 \frac{\partial \bar{U}}{\partial x}$ are associated with the production of \bar{u}^2 and that \bar{v}^2 appears through a transfer of energy from \bar{v}^2 through the pressure-velocity-gradient correlations (unless direct production of \bar{v}^2 is large).

5. DISCUSSION

A. The outer flow

Turbulent flows over irregular surfaces are usually scaled

with a friction velocity based on the drag of the fluid $u^* = (\tau_w / \rho)^{1/2}$. In many cases (Cohen & Hanratty [1968], Gill et al [1964]) the interpretation of measurements of mean velocity, with this scaling, produces von Karman constants larger than what is found for flow over a flat surface. The results presented in this paper could provide an explanation for this paradox and could raise some concern about the practice of using measurements of the average velocity to determine drag at a wavy gas-liquid interface^{14,15}.

Flow close to a train of steep solid waves experiences large variations in the direction of mean flow, at distances from the average location of the wave surface (y_0) of less than one reciprocal wave number ($2/\lambda$). Even though wave-induced flow variations are small in the outer flow, they are still large enough to make significant contributions to the transport of the momentum. A total fluid stress, τ_f , is therefore, defined as the sum of the wave-length average of the contributions of the mean flow and the turbulence (the Reynolds stress). An extrapolation, τ_f , to the average location of the wave surface gives the drag on the surface, or u^* . The measurements presented in this paper agree with measurements over a flat plate if they are sealed with friction velocity, u_w^* , obtained by extrapolating measurements of the Reynolds stress to y_0 .

This is of interest since the processes for producing turbulence at a wavy wall and at a flat wall are quite different. The results support the notion that the structure of stress producing motions in the outer flow could have a universal character, in that they are influenced by turbulence producing processes in the inner flow only through the magnitude of characteristic velocity u_w^* .

B. The inner flow

Turbulence production in the inner region for turbulent flow over a flat plate is associated with the flow oriented vortices attached to the wall (1993). Turbulence production, in the region for flow over a train of steep solid waves is fundamentally different. It is associated with a shear layer which is formed by the separation of the flow from the wave crest and which extends over the whole wavelength. This shear layer is the locus of a large production of turbulence and of large Reynolds stresses.

An understanding of turbulence close to the wall appears to require an understanding of how this shear layer interacts with the wall. Downstream of the crest, there exists a retarded flow which includes both a separated (on a time-mean basis) and non-separated regions. Turbulence in these regions is not set by local turbulence production; it is controlled by diffusion of turbulent kinetic energy from the shear layer. When the shear-layer is intercepted by the rising surface downstream of the trough a region of very large velocity gradients (a boundary-layer) is formed close to the surface. The interaction of turbulence formed by the shear layer with these large velocity gradients results in large turbulence production, in fact, the largest that is observed.

ACKNOWLEDGMENT

This work is being supported by the National Science Foundation under NSF CTS 92-00936.

REFERENCES

- J. W. Brooke and T. J. Hanratty, "Origin of turbulence-producing eddies in a channel flow," *Phys. Fluids*, **5**, 1011 (1993).
- J. J. Buckles, R. J. Adrian and T. J. Hanratty, "Turbulent flow over a large-amplitude wavy surface," *J. Fluid Mech.*, **27**, 140 (1984).
- F. H. Clauser, "Turbulent boundary layers in adverse pressure gradients," *J. Aeronaut. Sci.*, **21**, 91 (1954).
- L. S. Cohen and T. J. Hanratty, "Effect of waves at a gas-liquid interface on a turbulent air flow," *J. Fluid Mech.*, **31**, 467 (1968).
- K. A. Frederick and T. J. Hanratty, "Velocity measurements for a turbulent nonseparated flow over solid waves," *Exp. in Fluids*, **6**, 477 (1988).
- L. E. Gill, G. F. Hewitt, P. M. C. Lacey, "Sampling probe studies of the gas core in annular two-phase flow; Part 2. Studies of the effect of phase flow rates on phase velocity and velocity distribution," *Chem. Eng. Sci.*, **19**, 665 (1964).
- T. J. Hanratty and J. A. Campbell, Measurement of wall shear stress, in *Fluid Dynamics Measurements*, 2nd Edition, Hemisphere Publishing (1994).
- J. D. Hudson, "The effect of a wavy boundary on a turbulent flow," Ph.D. thesis, Univ. of Illinois, Urbana (1993).
- S. J. Kline and S. K. Robinson, "Turbulent boundary layer structure: Progress, status, and challenges," *Proceedings of the 2nd IUTAM Symposium on Structure of Turbulence and Drag Reduction* (Fed. Institute of Technology, Zurich, Switzerland, 1989).
- J. D. Kuzan, T. J. Hanratty and R. J. Adrian, "Turbulent flows with incipient separation over solid waves," *J. Fluid Mech.*, **7**, 88 (1989).
- J. W. McLean, "Computation of turbulent flow over a moving wavy boundary," *Phys. Fluids*, **26**, 2065 (1983).
- M. A. Niederschulte, "Turbulent flow through a rectangular channel," Ph.D. thesis, Univ. of Illinois, Urbana (1988).
- M. A. Niederschulte, R. J. Adrian and T. J. Hanratty, "Measurements of turbulent flow in a channel at low Reynolds numbers," *Exp. in Fluids*, **9**, 222 (1990).
- H. Schlichting, "Boundary-layer theory," p. 615, McGraw-Hill Series in Mechanical Eng., 7th edition (1979).
- D. P. Ziker and T. J. Hanratty, "Influence of the amplitude of a solid wavy wall on a turbulent flow. Part 2. Separated flows," *J. Fluid Mech.*, **90**, 257 (1979).

* Work performed at the University of Illinois. Pacific Northwest Laboratory is operated for the U.S. Department of Energy by Battelle Memorial Institute under Contract DE-AC06-76RLO1830.

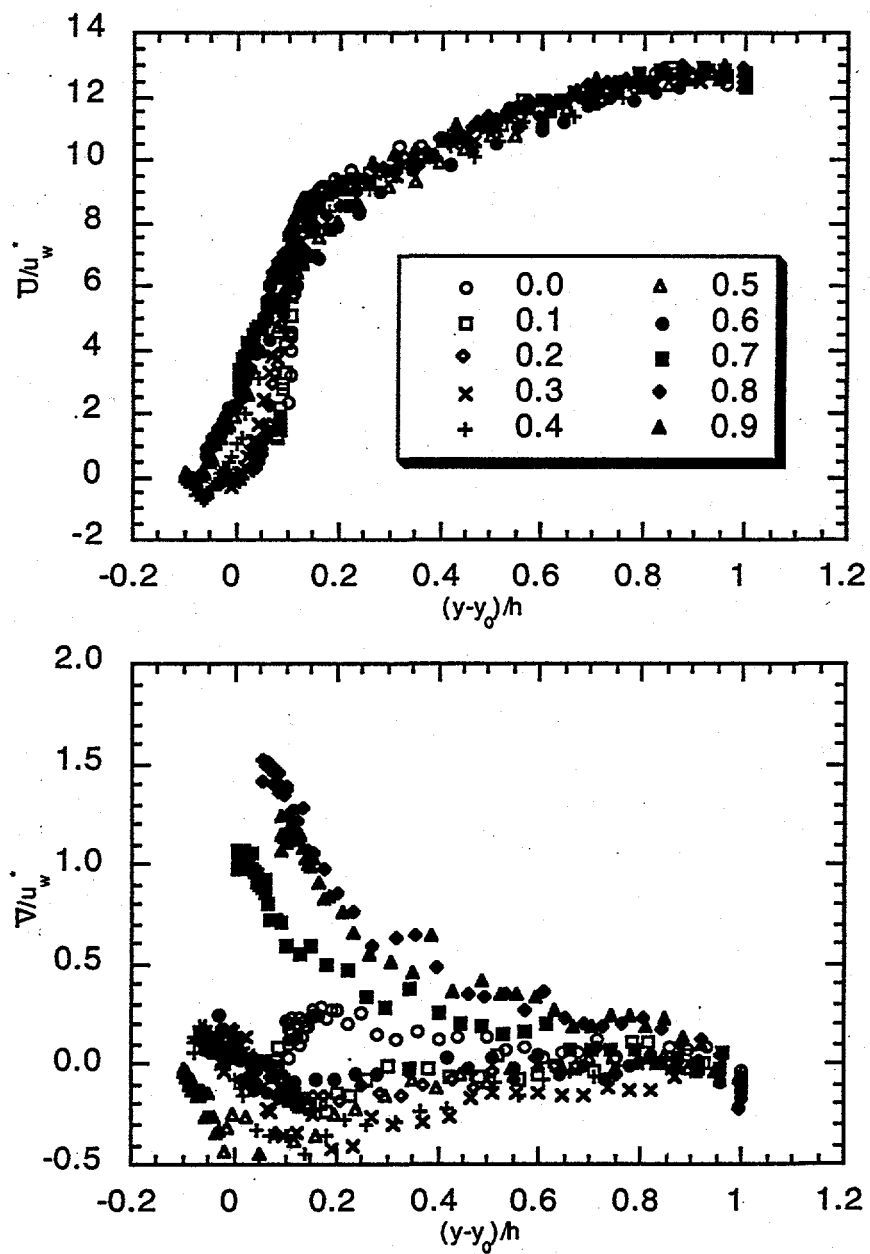


Figure 1 The mean streamwise (top) and normal (bottom) velocity profiles.

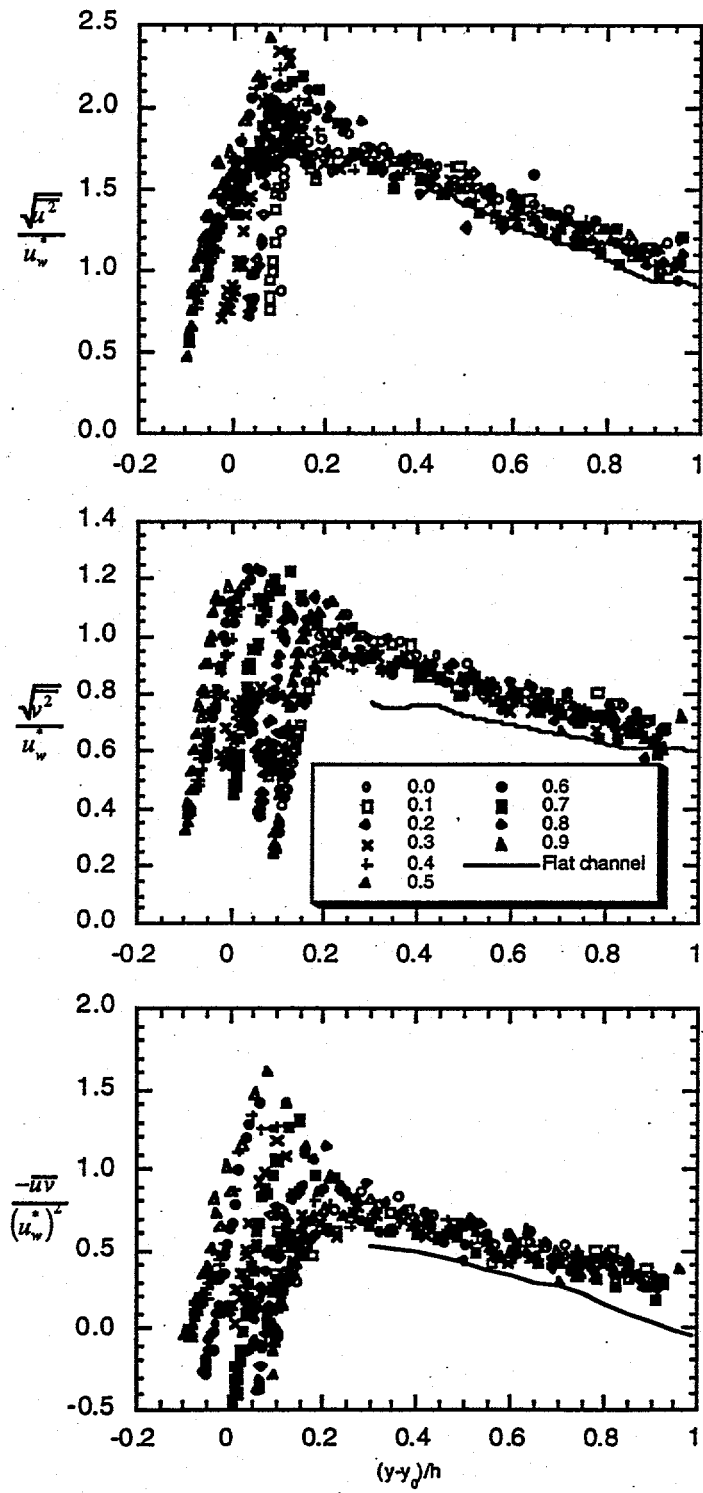


Figure 2 Profiles of the mean streamwise (top), normal (middle) turbulent velocity fluctuations and the mean Reynolds stress (bottom). Curves plot the data of Niederschulte, et al. (year) obtained in a flat channel.

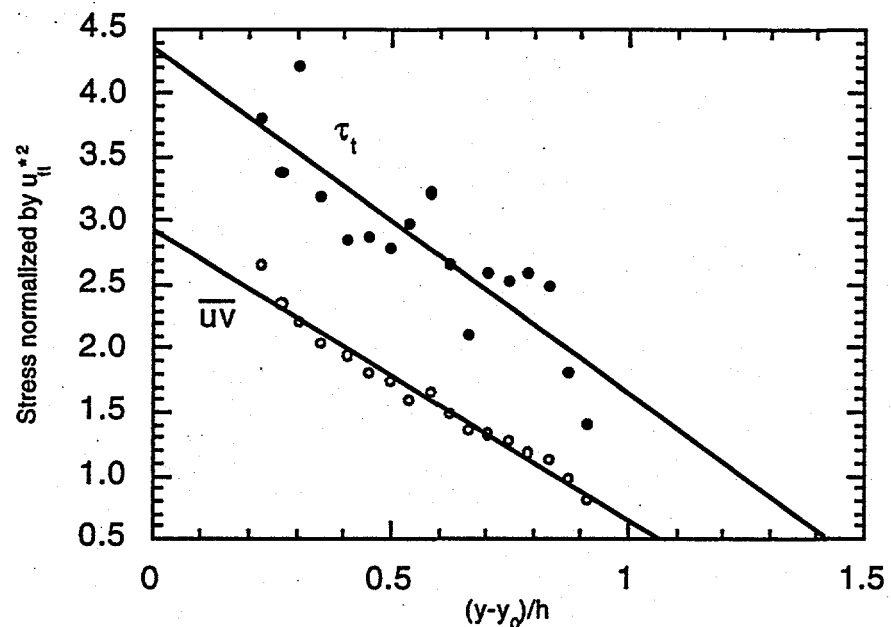


Figure 3 Wave-averaged shear stress profiles. These include the sum of the viscous shear stress (o) and the sum of the viscous shear stress, the Reynolds shear stress and the mean momentum transport term (*).

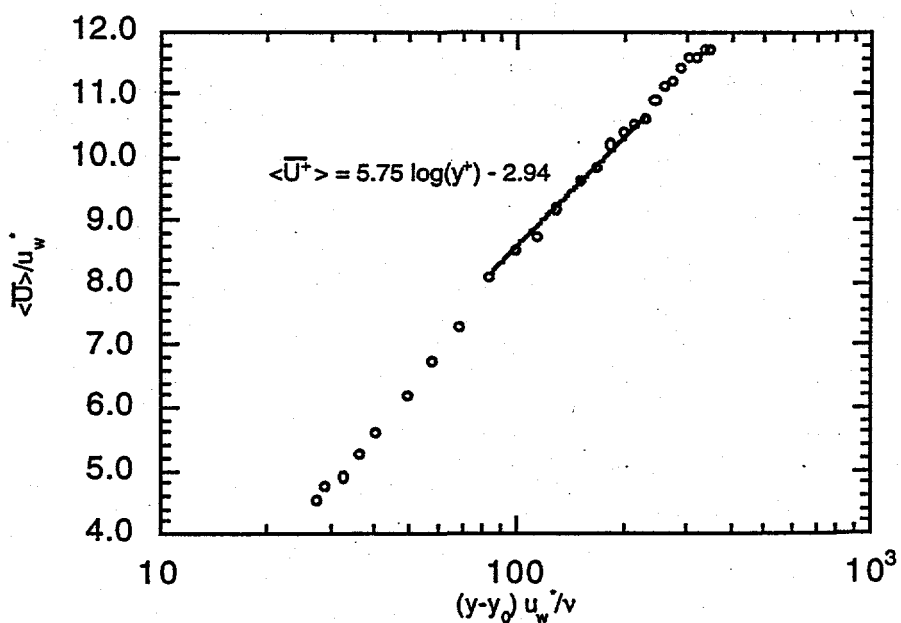


Figure 4 Wave-averaged mean streamwise velocities near the log-law region of the outer flow.

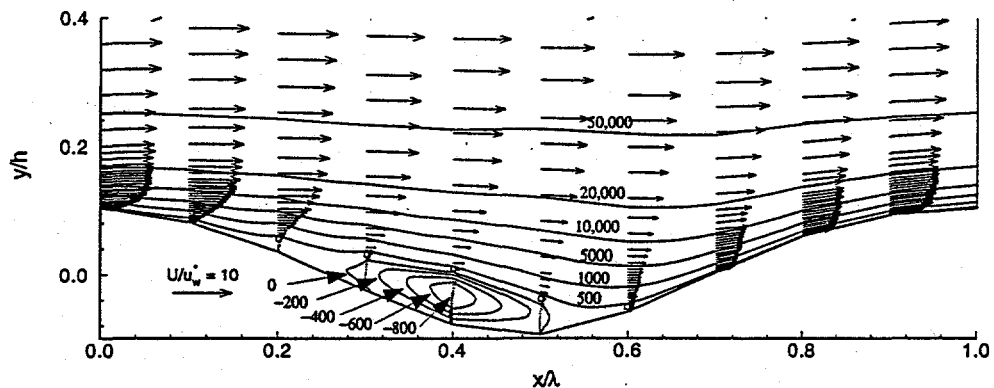


Figure 5 The mean velocity field with streamlines.

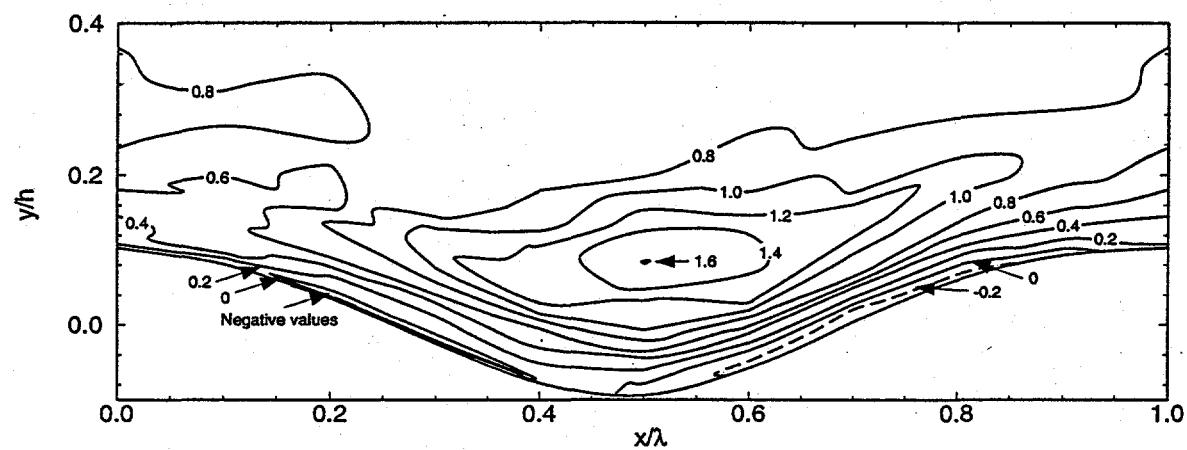


Figure 6 Contours of Reynolds shear stress.

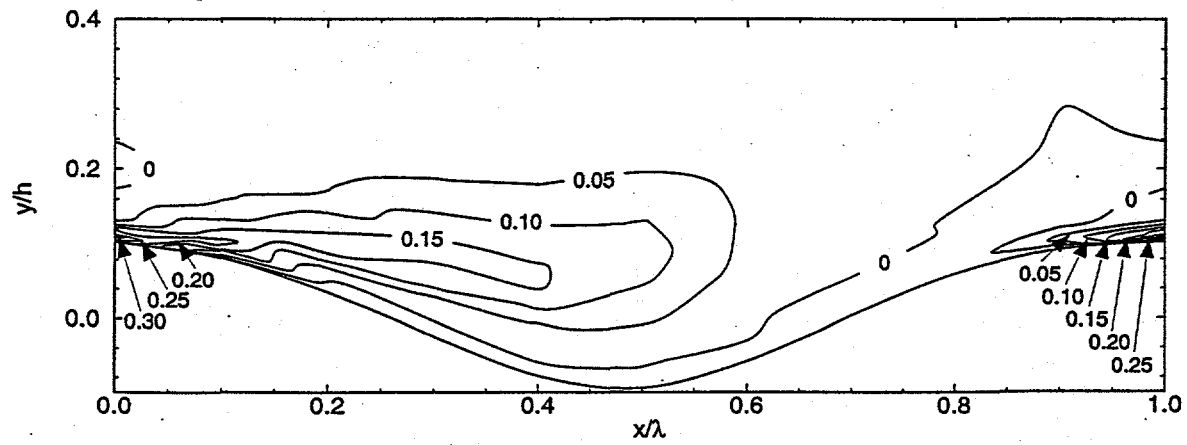


Figure 7 Turbulent kinetic energy production contours. The production is made dimensionless with u_w^{*4} / ν .

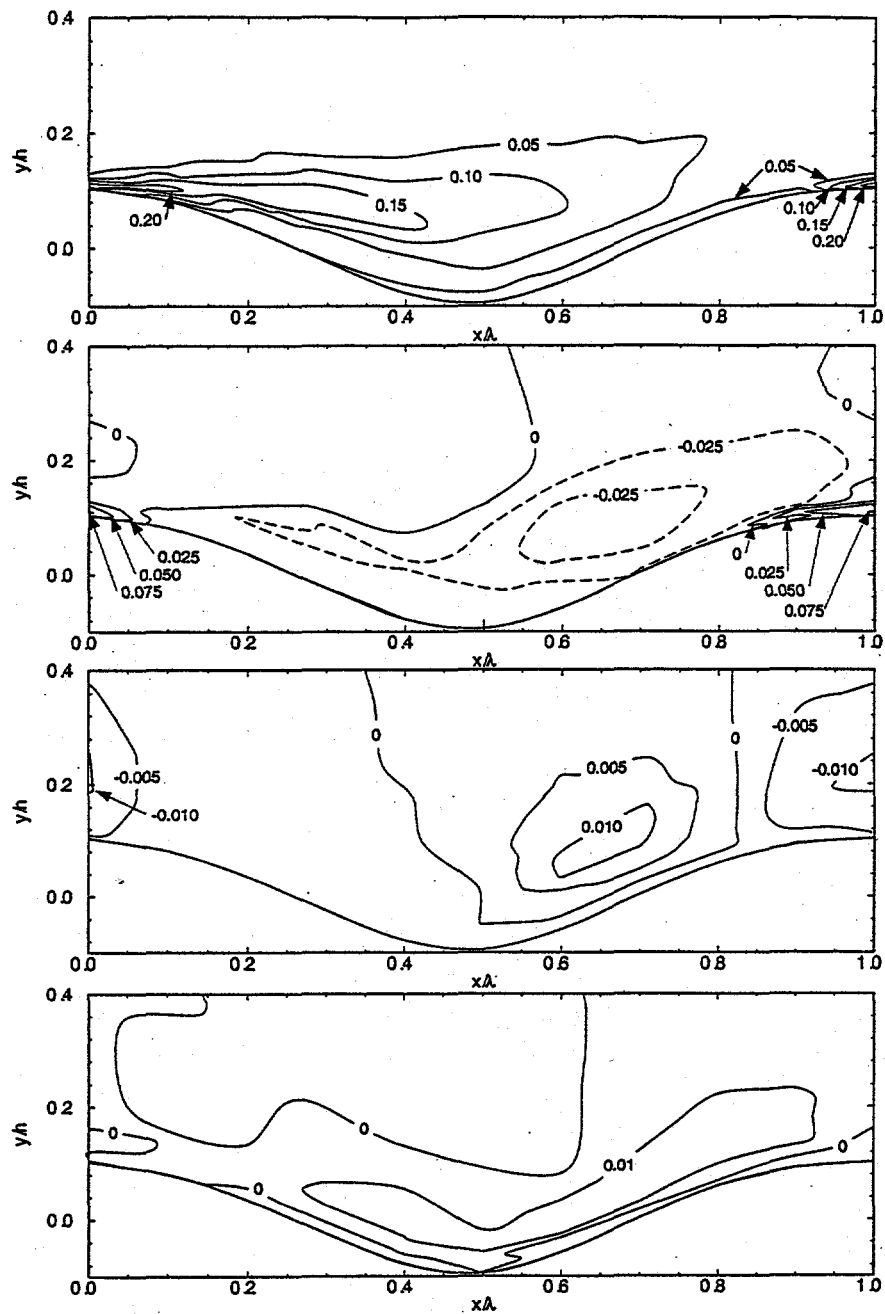


Figure 8 Contours of the four production terms. Contours of the (top to bottom) first production term, $-\bar{u}\bar{v}\frac{\partial \bar{U}}{\partial y}$; the second production term, $-\bar{u}^2\frac{\partial \bar{U}}{\partial x}$; the third production term, $-\bar{u}\bar{v}\frac{\partial \bar{V}}{\partial x}$; and the fourth production term, $-\bar{v}^2\frac{\partial \bar{V}}{\partial y}$. Units are made dimensionless with u_w^{*4} / ν .

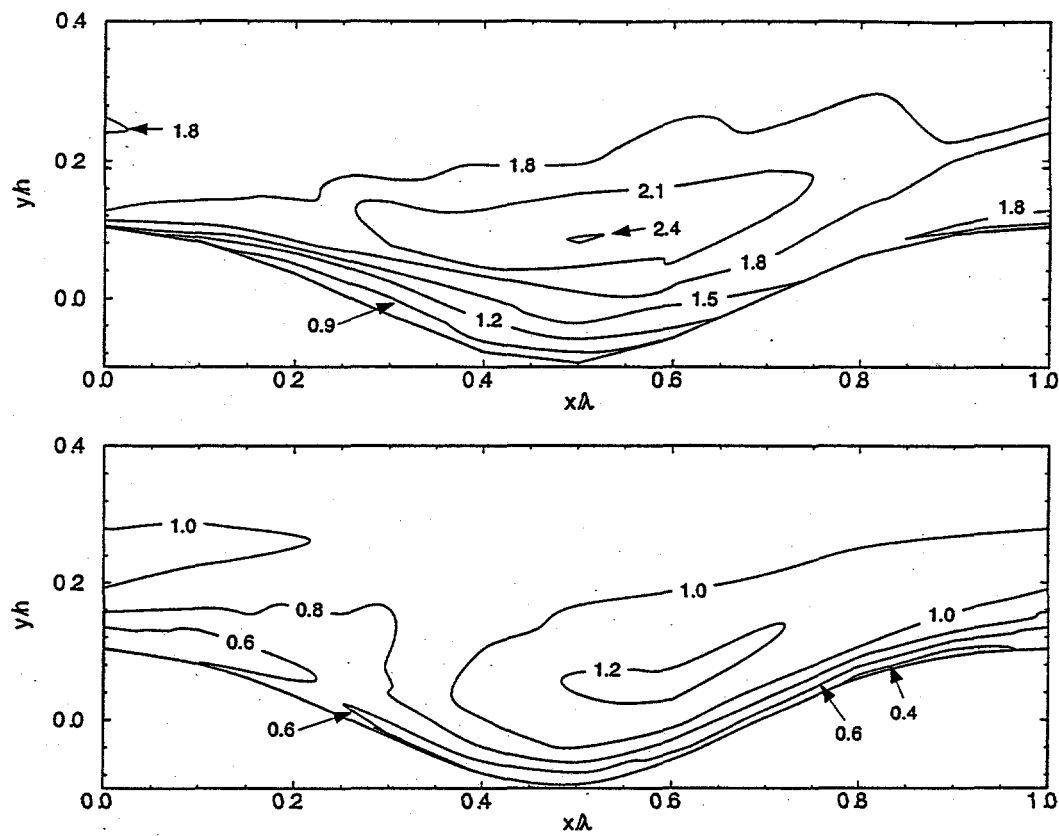


Figure 9 Contours of the mean streamwise $\sqrt{\bar{u}^2}$ (top) and normal $\sqrt{\bar{v}^2}$ (bottom) turbulent velocity fluctuations normalized by u_w^* .